Joint torque control for two-inertia system with encoders on drive and load sides

Shota Yamada*, Kenji Inukai*, Hiroshi Fujimoto**
The University of Tokyo
5-1-5, Kashiwanoha, Kashiwa, Chiba, 227-8561 Japan
Phone: +81-4-7136-3873*, +81-4-7136-4131**
Fax: +81-4-7136-3881*, +81-4-7136-4132**
Email: [yamada,inukai]@hflab.k.u-tokyo.ac.jp,
fujimoto@k.u-tokyo.ac.jp

Kenji Omata, Yuki Takeda, Susumu Makinouchi
Nikon Corporation
471, Nagaodaityou, Sakae, Yokohama, 244-8533 Japan
Email: Kenji.Omata@nikon.com, Yuki.Takeda@nikon.com,
Susumu.Makinouchi@nikon.com

***Abstract*—In the past 20 years, control methods for two-inertia systems have gradually changed from semi-closed control to full-closed control in order to achieve higher precision positioning. Though there is a trend toward the expansion of the use of load-side encoders in the industry, we can hardly say that control methods using load-side information are sufficiently studied. This paper proposes a novel joint torque control method for a two-inertia system using a high-resolution encoder on the load side. The proposed method enables us to control joint torque precisely considering nonlinear elements such as backlash, lost motion etc. Simulation and experimental results demonstrate that the good performance can be obtained by the proposed method.**

I. INTRODUCTION

Thanks to their reduction in cost, encoders have become widely used in various industrial fields. In the past, semi-closed control, which feeds back drive-side encoder's information, has often been applied in controlling industrial robots, machine tools, and welfare robots [1], [2]. In semi-closed control, however, shaft torsion between the motor and the load deteriorates positioning accuracy of the load side, where high-precision positioning is usually required. In order to achieve a precise position at the load side, full-closed control, which feeds back load-side information as well as drive-side information has been widely studied. Therefore, the number of machine tools having encoders at the load side is increasing.

As for industrial robots, it is usually difficult to equip with encoders at the load side due to the lack of space for mounting an encoder and the scattering of lubricant. In this paper, we propose a novel machine structure to compact both the drive-side and load-side encoders, and utilize it to an industrial robot module. The device was developed with the aim of improving the accuracy of positioning at the load side. Like this, there is a trend expanding the use of load-side encoders in the industry, but we can hardly say that control methods using load-side information have been sufficiently studied.

This awareness of the problem has encouraged our research group to propose novel control methods using load-side information [3], [4], [5]. It can be imaginable that the use of encoders at the load side is going to expand thanks to the reduction in cost of encoders. Therefore, novel control methods for the system with encoders at both the drive and load side are highly required.

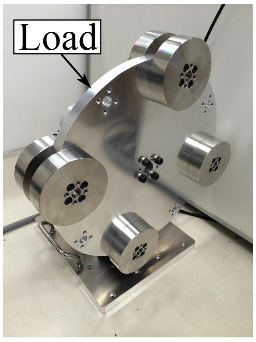

(a) DEMCM(Load side)

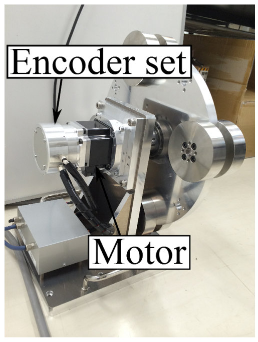

(b) DEMCM(Drive side)

Fig. 1. Overviews of DEMCM.

This paper proposes a novel joint torque control method for a two-inertia system using a high-resolution encoder on the load side. Joint torque is the torque of transmission between the motor and the load. The joint torque control means the control of the torque directly driving the load. Therefore, the precise joint torque control makes many things possible, for example: complicated tasks such as assembling, improvements of convenience and safety of users, and high backdrivability [6], [7]. The proposed method enables us to control joint torque precisely considering nonlinear elements such as backlash, lost motion etc, which are often ignored in conventional joint torque control methods. The advantage of the proposed method will be demonstrated in simulations and experiments.

II. EXPERIMENTAL DEVICE

The experimental device, named as Double Encoders Motion Control Module (DEMCM), is developed aiming at the application to industrial robots. The overviews of DEMCM are shown in Fig. 1(a) and 1(b). Conventionally, it has been difficult to equip industrial robots with an encoder at the load side due to the lack of space and the scattering of lubricant. As shown in Fig. 2, the device has a structure that can solve the

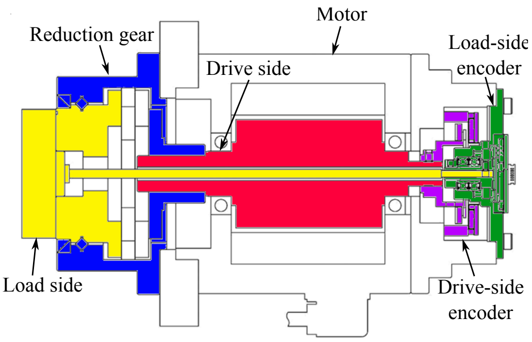

Fig. 2. Structure of DEMCM.

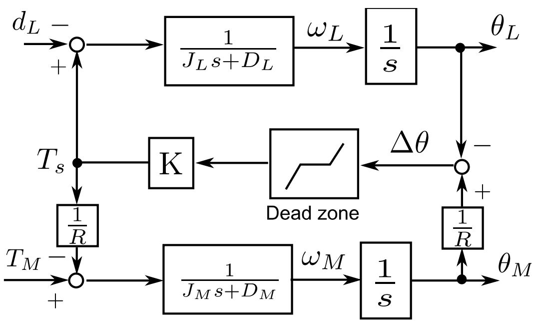

Fig. 3. Block diagram of a two-inertia model of DEMCM.

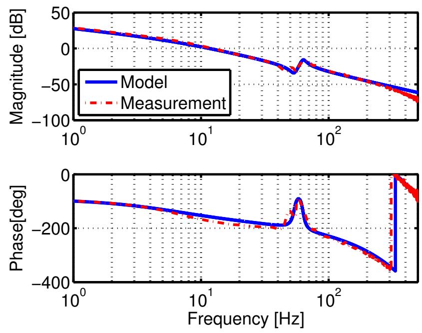

Fig. 4. Frequency responses from drive-side input torque to drive-side angle.

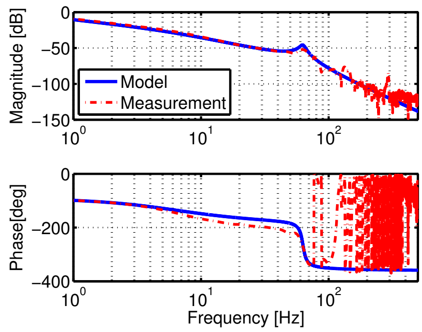

Fig. 5. Frequency responses from drive-side input torque to load-side angle.

aforementioned problems. There is an output shaft between the load and the load-side encoder through the hollow motor, and the drive-side encoder and the load-side encoder are equipped side by side. The load-side encoder enables us to achieve more precise positioning compared with semi-closed control by considering the influence of shaft torsion.

The mechanical resonance frequency of the output shaft is sufficiently high because the shaft has high rigidity and the moment of inertia of the load-side encoder is very small. The transfer characteristic of the shaft has little effect on the whole system's characteristic. Therefore, the whole system can be modeled as a two-inertia system composed of the motor, the reduction gear, and the load.

III. TWO-INERTIA SYSTEM MODELING

Fig. 3 shows the block diagram of the device modeled as a two-inertia system. Let angle, angular velocity, torsional rigidity, moment of inertia, viscosity friction coefficient be θ, ω, K, J, D, respectively. Suffix $_M$ denotes the motor side (or the drive side). On the other hand, suffix $_L$ means the load side. T_M, d_L, T_s, $\Delta\theta$, $\Delta\omega$, and R indicate input torque, load-side disturbance, joint torque, torsional angle, torsional angular velocity, and reduction ratio, respectively.

The device uses a harmonic reduction gear and it includes some nonlinear elements [8]. In the block diagram, backlash, which is one of nonlinear elements existing in the device, is modeled as dead zone.

The measured frequency characteristic of the transfer function from the input torque to the drive-side angle of the device is indicated in Fig. 4 and the frequency characteristic of the transfer function from the input torque to the load-side angle is indicated in Fig. 5 with the dashed line. It is observed that the device has mechanical resonance at 67 Hz.

The frequency characteristics shown in Fig. 4, 5 are fitted by a two-inertia model. Solid lines indicate the characteristics of the fitted model. The identified parameters are shown in Tab. 1.

IV. JOINT TORQUE CONTROL

A. *Conventional joint torque control methods*

Conventional joint torque control methods are classified broadly into two groups, the methods using torque sensors [9], [10] and the methods using reaction force observer(RFOB) [11], [12]. Using torque sensors bring demerits such as lowering the system rigidity, high cost, low bandwidth of torque sensors, and bad effects due to sensors' noises [13]. The methods using RFOB can avoid the demerits. Therefore RFOB is applied in the proposed method.

B. *Usefulness of joint torque control*

The joint torque control makes many things possible, for example: complicated tasks such as assembling, improvements of convenience and safety of users [6], [7]. Moreover, the precise joint torque control enables us to enhance backdrivability. Backdrivability is a mobility of the system composed of the actuator and the load when the load is forced to move.

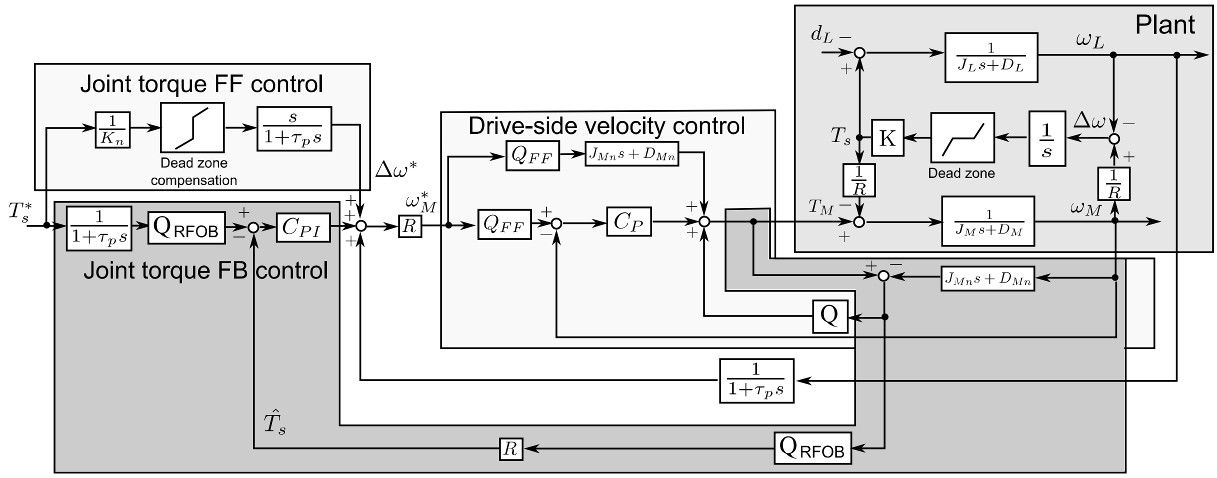

Fig. 6. Block diagram of the proposed method.

TABLE I
PARAMETERS OF DEMCM.

Motor-side moment of inertia J_M	1.2e-4	kgm^2
Motor-side viscosity friction coefficient D_M	5.0e-3	Nms/rad
Torsional rigidity coefficient K	3.2e+4	Nm/rad
Load-side moment of inertia J_L	2.8e-1	kgm^2
Load-side viscosity friction coefficient D_L	1.0e+1	Nms/rad
Reduction ratio R	80	

Usually the reduction gears decrease the backdrivability of the system. Enhancing the backdrivability benefits users in various fields, especially in the environment where machines and human work together.

In the field of wearable robots, where the backdrivability is highly required, Series Elastic Actuator (SEA) is often applied [14], [15]. Generally speaking, low-rigid elements in a system deteriorate control performance, and it is desirable for the system to have higher rigidity for higher control bandwidth [16]. Therefore, SEA can be regarded as an actuator that acquires high backdrivability by having elastic springs at the expense of control performance.

V. PROPOSED JOINT TORQUE CONTROL

A. Outline of proposed method

Based on a trend expanding the use of load-side encoders in the industry due to strong demand for high precision positioning, this paper proposes a joint torque control method for two-inertia systems with load-side encoders. Utilizing both drive and load side information enable us to control torsional angular velocity, and this can make precise joint torque control possible. Moreover, torsional angular velocity control enables us to design feed forward (FF) controller considering nonlinear elements at transmission mechanisms such as backlash and nonlinear springs etc, which are often ignored in conventional joint torque control methods. The proposed method does not need a torque sensor, which has the demerits, or a hardware change like SEA, but enables us to achieve high backdrivability of servo motors with reduction gears by utilizing the load-side information effectively.

Fig. 6 shows a block diagram of the proposed method. The symbols in the block diagram indicate the following: C_P: P controller of drive-side angular velocity, C_{PI}: PI controller of joint torque, $\hat{T}_s$: joint torque estimated by RFOB, Q: low pass filter(LPF) of disturbance observer(DOB), Q_{RFOB}: LPF of RFOB, Q_{FF}: the 1st order LPF to make angular velocity FF control proper, τ_p: time constant of pseudo differential. Suffix $_n$ denotes nominal values and superscript * means reference values. The proposed method can be divided into three parts.

B. Drive-side angular velocity control for torsional angular velocity control

The proposed method controls joint torque by controlling torsional angular velocity. For torsional angular velocity control, collocated drive-side angular velocity is controlled and then combined with the load-side angular velocity obtained by a load-side encoder. Here, from Fig. 6 the torsional angular velocity $\Delta\omega$ is obtained as (1).

$$\Delta\omega = \frac{\omega_M}{R} - \omega_L \tag{1}$$

Therefore, the reference value of the drive-side angular velocity can be generated as (2) by using the reference value of the torsional angular velocity and the load-side angular velocity.

$$\omega_M^* = R(\Delta\omega^* + \omega_L) \tag{2}$$

The drive-side angular velocity is controlled by DOB and a P controller. The drive-side angular velocity FF controller is also applied to achieve a high control bandwidth. A higher control bandwidth of the inner loop control improves the response of the outer loop. The drive-side angular velocity FF controller is implemented as $(J_{Mn}s + D_{Mn})$ on the assumption that the reaction joint torque is decoupled. Then the first order LPF Q_{FF} is applied to make $(J_{Mn}s + D_{Mn})$ proper.

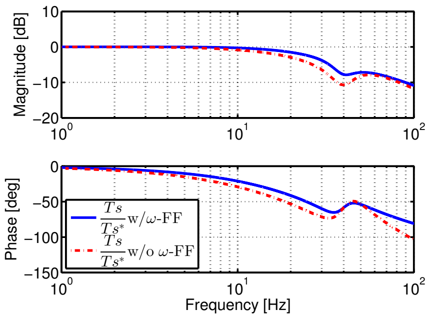

Fig. 7. Bode plots of closed-loop characteristics of joint torque control.

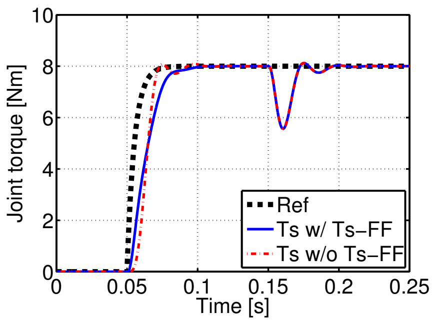

Fig. 8. Step responses of joint torque with and without joint torque FF.

C. Joint torque FF control

The joint torque FF control part generates the reference value of the drive-side angular velocity from the reference value of the joint torque. Considering an inverse model from $\Delta\omega$ to T_s shown in Fig. 3, the reference value of the drive-side angular velocity is generated using the reciprocal of the torsional rigidity, the inverse model of nonlinear elements, and the derivative. The derivative is implemented as pseudo differential with time constant τ_p. In this paper, backlash is modeled as a dead zone, so the inverse model of the dead zone is applied for nonlinear compensation.

D. Joint torque FB control

The joint torque FB control part controls the estimated joint torque with a PI controller. The PI controller is designed by the pole placement to the plant, $T_s = \frac{k}{s}\Delta\omega$. The PI control enables us to control joint torque without state steady error. Considering the delay of Q_{RFOB}, Q_{RFOB} is also applied to the reference value of the joint torque.

VI. SIMULATION

The performance of the proposed method is evaluated in simulations. The simulation model is the two-inertia system model with the identified parameters of Tab.1. For the sake of simplification of simulations, it is assumed that nonlinear elements in the plant model are not included if not specified.

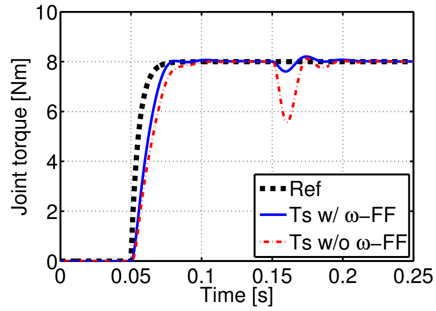

Fig. 9. Step responses of joint torque with and without angular velocity FF.

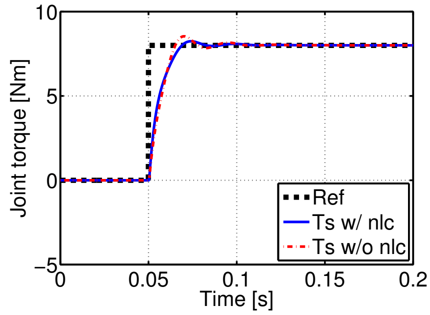

Fig. 10. Step responses of joint torque with and without nonlinear compensation.

A. Designing controllers

The drive-side angular velocity P controller is designed such that its control bandwidth becomes 180 Hz. The cut-off frequency of DOB and RFOB are set as 30 Hz. The cut-off frequency of Q_{FF} and the pseudo differential are 1 kHz. These values are determined experimentally considering modeling errors and noises.

The PI controller for the joint torque is designed such that the two poles are placed at 30 Hz. There is an assumption that torque sensors are not used, so the joint torque obtained in experiments is an estimated torque by the reaction force observer. Therefore, the characteristics of the estimated torque is studied. Note that in simulations there are no modeling errors in the observers or in the FF models.

B. Simulation results

The bode plots of the closed-loop characteristics of the joint torque control are shown in Fig. 7. The solid line indicates the response with angular velocity FF control while the dashed line indicates that without FF control. By applying FF control to the inner loop angular velocity control, the control bandwidth of the joint torque response increases from 20 Hz to 27 Hz.

Fig. 8 shows the comparison of the step responses of the joint torque with and without joint torque FF control when angular velocity FF control is not applied. The 8 Nm step reference with the first order LPF whose cut-off frequency is 30 Hz is input at 0.050 s and a -10 Nm step load-side

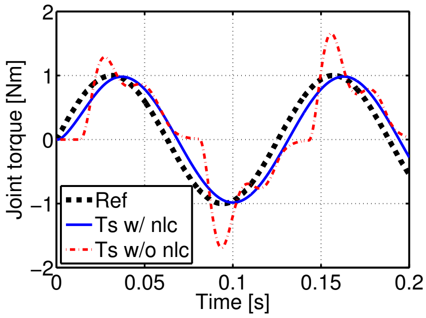

Fig. 11. Sin responses of joint torque with and without nonlinear compensation.

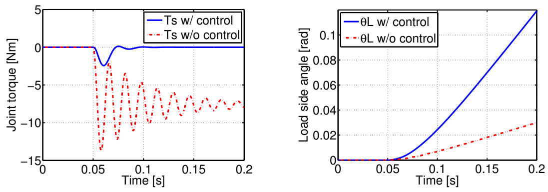

(a) Joint torque.

(b) Load-side angle.

Fig. 12. Realization of backdrivability(comparison with the proposed control and without any control when the load-side step disturbance is input).

disturbance is also input at 0.15 s. The dotted line indicates the reference value and the solid line indicates the response with joint torque FF control while the dashed line indicates the response without joint torque FF control. The joint torque FF control improves the responsiveness at starting while without FF control the response has a slight vibration. As for the disturbance response, there is no difference between the response with and without joint torque FF control.

Fig. 9 shows the comparison of the step responses of the joint torque with and without angular velocity FF control when joint torque FF control is applied. With angular velocity FF control the responsiveness and the disturbance suppression performance are improved.

A comparison of the step responses of the joint torque with and without nonlinear compensation is shown in Fig. 10. In this simulation, nonlinear elements are modeled as a dead zone, and the width of the dead zone is set as the maximum backlash width (5.3e-5 rad) written in the specification sheet of the gears equipped in the setup. The initial position is at the center of the backlash. With nonlinear compensation, vibration is suppressed and control performance is improved.

Moreover, to study the response at the velocity reversal point, sinusoidal responses are shown in Fig. 11. The amplitude of the sinusoidal reference is 1 Nm and the angular frequency is 50 rad/s. Without nonlinear compensation, only the amplitude of the initial response is relatively small, due to the initial position being at the center of the backlash, and thus reducing the effect of nonlinear elements to half of that at the velocity reversal. With nonlinear compensation control, the performance is clearly improved. In this simulation, the

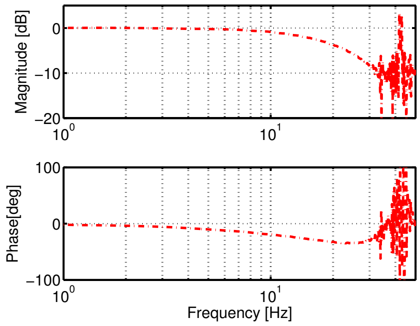

Fig. 13. Frequency response of closed-loop characteristic of joint torque control in experiment.

perfect precise inverse model of nonlinear elements in the plant is used, but it is difficult to model nonlinear elements in real plant precisely. Therefore, it is important to model nonlinear elements in the plant such that it represents nonlinear characteristics precisely and it has an inverse model.

Finally, simulations about backdrivability are shown in Fig. 12(a) and 12(b). The joint torque reference is 0 Nm and a -10 Nm step load-side disturbance is input at 0.050 s. The solid line indicates the response with the proposed control while the dashed line indicates the response without any control. The proposed method enables the joint torque to be 0 Nm in about 0.050 s. Fig. 12(b) shows that with the proposed method, the load-side angle moves more with the same amount of the load-side disturbance, meaning that the proposed method realizes backdrivability free from drive-side friction.

VII. EXPERIMENT

The gains and structures of the controllers are the same as those in the simulations. The controllers are discretized by Tustin conversion and the sampling period is 0.20 ms. Angular velocity is obtained by a backward difference of angle with the first order LPF whose cut-off frequency is 1 kHz.

The frequency response of closed-loop characteristic of the joint torque control in the experiment is shown in Fig. 13. This is the case of the response without angular velocity FF control, so in the simulation this corresponds to the dashed line in Fig. 7. Fig. 13 shows that the control bandwidth is 18 Hz. This slight decrease of control bandwidth is considered to be due to modeling errors.

Experimental comparisons of the step responses of the joint torque are shown in Fig. 14 and 15. In Fig. 14 the dotted line indicates the reference value and the solid line indicates the response with joint torque FF control while the dashed line indicates the response without joint torque FF control. This experimental comparison corresponds to Fig. 8 in the simulation. Fig. 14 shows that as in the simulation the responsiveness at starting is improved with joint torque FF control.

In Fig. 15 the dotted line indicates the reference value and the solid line indicates the response with angular velocity FF control while the dashed line indicates the response without

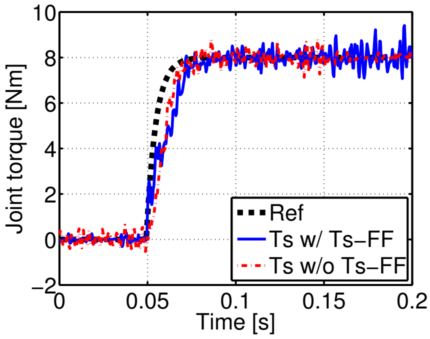

Fig. 14. Experimental comparison of step responses of joint torque with and without joint torque FF control.

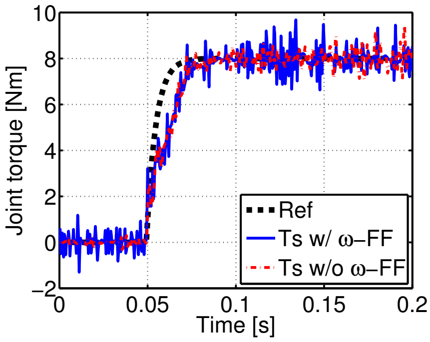

Fig. 15. Experimental comparison of step responses of joint torque with and without angular velocity FF control.

angular velocity FF control. This experimental comparison corresponds to Fig. 9 in the simulation. In the experiment there is not a clear difference between the response with and without angular velocity FF control. This can be considered to be caused by the sensor noise and modeling error. With angular velocity FF control the response has much noise. This is because by adding FF control to the inner loop, noise caused by joint torque estimation with the sensor noise and modeling error has much more effect. Though the addition of FF control to the inner loop can improve the control performance theoretically, you need to consider about the sensor noise and modeling errors.

VIII. CONCLUSION

In this paper, considering a trend expanding the use of load-side encoders in the industry, a joint torque control method using both drive-side and load-side encoders is proposed. Joint torque control for a two-inertia system makes complicated tasks possible by robots and machine tools. The controllers of the proposed method are designed and the performance is evaluated in simulations and experiments.

Though in this paper simple nonlinear compensation using an inverse model of dead zone is applied, nonlinear compensation considering initial position obtained by encoders on the drive and load side will be studied. Because it is difficult to input the precise load-side disturbance, experiments on disturbance suppression and backdrivability are not conducted. Therefore, these experiments will be studied in other setups. Moreover, only zero or step was input and considered as the reference value of joint torque, but more advanced control such as impedance control or contact detection can be applied in the future.

REFERENCES

[1] J. Hu and F. Hu:"Analysis and Design to the Asymptotic Behavior of the Semi/Full/Dual-closed Loop Feedback Position Control System", *Proc. SICE Annu. Conf., Akita, Aug. 2012*, pp. 1096–1101.

[2] Z. Jamaludin, H. Van Brussel, and J. Swevers:"Friction Compensation of an XY Feed Table Using Friction-Model-Based Feedforward and an Inverse-Model-Based Disturbance Observer", *Trans. IEEE on Industrial Electronics*, vol. 56, no. 10, pp. 3848–3853, 2009.

[3] M. Aoki, H. Fujimoto, Y. Hori and T. Takahashi:"Robust Resonance Suppression Control based on Self Resonance Cancellation Disturbance Observer and Application to Humanoid Robot", *Proc. IEEE Int. Conf. on Mechatronics (ICM), Vicenza, Feb./Mar. 2013*, pp. 623–628.

[4] K. Sakata, H. Asaumi, K. Hirachi, K. Saiki, and H. Fujimoto:"Self Resonance Cancellation Techniques for a Two-mass and its application to a Large-Scale Stage", *IEEJ Trans. on Ind. Appl.*, vol. 3, no. 6, pp. 455–462, 2014

[5] S. Yamada, H. Fujimoto:"Vibration Suppression Control for a Two-Inertia System using Load-Side High-Order State Variables Obtained by a High-Resolution Encoder", *Proc. 40th Annu. Conf. IEEE Ind. Electron. Soc. (IECON)*, Dallas, Oct./Nov. 2014, pp. 2897-2903

[6] B. Na, J. Bae, and K. Kong:"Back-drivability recovery of a full lower extremity assistive robot", *Proc. 12th Int. Conf. IEEE on Control, Automation and Systems (ICCAS), JeJu Island, Oct. 2012*, pp. 1030–1034.

[7] P. Weiss, P. Zenker, and E. Maehle:"Feed-forward Friction and Inertia Compensation for Improving Backdrivability of Motors", *Proc. 12th Int. Conf. IEEE on Control, Automation, Robotics and Vision (ICARCV), Guangzhou, Dec. 2013*, pp. 288–293.

[8] M. Yamamoto, M. Iwasaki, M. Kainuma, Y. Okitsu, K. Yuki, K. Sasaki, T. Yajima:"Compensation for Synchronous Component of Angular Transmission Errors in Harmonic Drive Gearings", *Proc. 11th IEEE Int. Workshop on Advanced Motion Control (AMC), Nagaoka, Mar. 2010*, pp. 361–365.

[9] T. Kawakami, K. Ayusawa, H. Kaminaga, and Y. Nakamura:"High–Fidelity Joint Drive System by Torque Feedback Control Using High Precision Linear Encoder", *Proc. IEEE Int. Conf. on Robotics and Automation (ICRA), Anchorage, May. 2010*, pp. 3904–3909.

[10] Y. Kuroki, Y. Kosaka, T. Takahashi, E. Niwa, H. Kaminaga, and Y. Nakamura:"Cr–N Alloy Thin–film Based Torque Sensors and Joint Torque Servo Systems for Compliant Robot Control", *Proc. IEEE Int. Conf. on Robotics and Automation (ICRA), Karlsruhe, May. 2013*, pp. 4954–4959.

[11] S. Oh and Y. Hori:"Generalized Discussion on Design of Force-sensor-less Power Assist Control", *Proc. 10th Int. Workshop on Advanced Motion Control (AMC), Trento, Mar. 2008*, pp. 492–497.

[12] C. Mitsantisuk, M. Nandapaya, K. Ohishi, and S. Katsura:"Design for Sensorless Force Control of Flexible Robot by Using Resonance Ration Control Based on Coefficient Diagram Method", *Automatika*, vol. 54, no. 1, pp. 62–73, 2013.

[13] S. Katsura, Y. Matsumoto, and K. Ohnishi:"Modeling of Force Sensing and Validation of Disturbance Observer for Force Control", *IEEE Trans. on Industrial Electronics*, vol. 54, no. 1, 2007.

[14] N. Paine, S. Oh, and L. Sentis:"Design and Control Considertaions for High-Performance Series Elastic Actuator", *IEEE Trans. on Mechatronics*, vol. 19, no. 3, 2014.

[15] K. Kong, J. Bae, and M. Tomizuka:"A Compact Rotary Series Elastic Actator for Human Assistive Systems", *IEEE Trans. on Mechatronics*, vol. 17, no. 2, 2012.

[16] R. van Herpen, T. Oomen, E. Kikken, M. van de Wal, W. Aangenent, and M. Steinbuch:"Exploiting Additional Actuators and Sensors for Nano-Positioning Robust Motion Control", *Proc. American Control Conf., Portland, Jun. 2014*, pp. 984–990.